

Hepatitis Virus Protein X-Phenylalanine Hydroxylase fusion proteins identified in PKU mice treated with AAV-WPRE vectors

Research Article

Jennifer E. Embury^{1,*}, Susan Frost¹, Catherine E. Charron³, Emilio Madrigal¹, Omaththage Perera⁵, Amy E. Poirier², Andreas G. Zori¹, Russ Carmical⁴, Terence R. Flotte⁶, Philip J. Laipis¹

¹Department of Biochemistry and Molecular Biology

²Department of Pediatrics, University of Florida, Gainesville, Florida 32610, USA

³National Heart and Lung Institute, Imperial College School of Medicine, London, United Kingdom

⁴University of Texas Medical Branch, Galveston, Texas 77555, USA

⁵Southern Insect Management Research Unit, Agricultural Research Service, USDA, Stoneville, Mississippi 38776, USA

⁶School of Medicine, University of Massachusetts, Worcester, Massachusetts 01655, USA

*Correspondence: Jennifer E. Embury, DVM, Dept. of Biochemistry and Molecular Biology, PO Box 100245, College of Medicine, University of Florida, Gainesville, FL 32610, USA; Tel: (352) 392-6493; Fax: (352) 392-1445; e-mail: jembury@ufl.edu

Key words: Hepatitis Virus Protein X, fusion proteins, AAV-WPRE vectors, Serum phenylalanine assay, DNA extraction, immunohistochemistry, Histopathology, sequencing and quantitative PCR, Plasmid, vector construction, Western blot analysis

Abbreviations: adeno-associated viral (AAV); Hepatitis B virus (HBV); Hepatitis B Virus X-protein (HBx); phenylalanine hydroxylase (PAH); post-transcriptional regulatory element (WPRE); woodchuck hepatitis virus (WHV)

The authors declare no competing financial interests.

Received: 16 April 2008; Revised: 4 June 2008

Accepted: 5 June 2008; electronically published: June 2008

Summary

Utilizing the *Pah*^{enu2} mouse model for phenylketonuria (PKU), we developed an improved expression vector containing the Woodchuck Hepatitis Virus post-transcriptional regulatory element inserted into a rAAV-mPAH construct (rAAV-mPAH-WPRE) for treatment of PKU. Following portal vein delivery of these vectors to *Pah*^{enu2} mice, we observed the unintentional development of neoplastic disease (44%) and hepatic pathology (70%) in WPRE-treated mice. Our vector contained a portion of the oncogenic hepadnoviral “X-protein” in the WPRE segment that had been intentionally modified in an attempt to prevent its expression. The hepadnoviral X-protein encoding sequence is known to function as a mediator in oncogenic activity (Murakami, 1999). We have evidence that the X-protein fragment unexpectedly formed a fusion protein with a phenylalanine hydroxylase transgene in our vector and suspect this fusion protein may have been responsible for the high rate of unusual types of cancer and hepatic pathology. These results are not to imply that the use of the WPRE element will always result in the development of cancer. But in this particular instance, an unanticipated event may have ensued when the X-protein formed a fusion protein with the transgene. This is a cautionary illustration to be considered when developing genetic therapies to treat diseases.

I. Introduction

A post-transcriptional regulatory element (WPRE) derived from the woodchuck hepatitis hepadnavirus has been utilized in numerous viral vectors to enhance transgene expression (Donello et al, 1998; Loeb et al, 1999; Zufferey et al, 1999). Our laboratory developed

adeno-associated viral (AAV) vectors containing a WPRE element and a phenylalanine hydroxylase (PAH) coding sequence for treatment of *Pah*^{enu2} phenylketonuric (PKU) mice based on previous work by Song and colleagues in 2001. Phenylketonuria (PKU) is a common human birth defect that occurs in approximately one in 16,000 births in

the United States. The disease is caused by a single gene defect in the enzyme phenylalanine hydroxylase (PAH) that results in hyperphenylalanemia and subsequent neurologic impairment (Shedlovsky et al, 1993; Scriver et al, 1995).

II. Materials and Methods

A. Plasmid and vector construction

The rAAV-mPAH vector was derived from p43CB-AAT by replacement of the AAT cDNA with the mPAH cDNA. The WPRE vector was constructed by inserting the WPRE and bovine growth hormone polyadenylation signal between the NotI and MfeI restriction sites replacing the original SV40 polyA signal. Recombinant virus production was performed as described previously (Song et al, 2001).

B. Serum phenylalanine assay

Serum samples were obtained from the tail vein and collected into heparinized capillary tubes. 7.5µl of serum was TCA precipitated and placed on ice for 10 minutes. Each sample was assayed in triplicate in a microtiter plate with 4µl of serum or standard with 64µl of cocktail (McCaman and Robins, 1962). After a 2-hour incubation at 60°C, 400µl of copper reagent was added followed by reading on an FLx800 Multidetector Microplate Reader (Bio Tek, Winooski VT).

C. Animals use and surgical procedures

Our colony of *Pah^{enu2}* mice is maintained and handled as approved by the University of Florida Institutional Animal Care and Use Committee (IACUC, Gainesville, FL). The *Pah^{enu2}* mouse model was initially created through ethylnitrosurea mutagenesis of BTBR mice (Shedlovsky et al, 1993). The mutation is a T to C transition changing Phe 263 to Ser, and incidentally creates a new *Alw261* restriction site in exon 7 of the PAH gene on chromosome 10 (McDonald and Charlton, 1997). The *Pah^{enu2}* mutation is confirmed by polymerase chain reaction (PCR) amplification of an exon 7 genomic fragment followed by digestion with *Alw261*.

All mice selected for gene therapy experiments were between 10 to 14 weeks old, and categorized into groups as previously described. Prior to portal vein surgical procedures, all animals were anesthetized with 3% isoflurane, and surgeries were performed on a thermoregulated operating board. The portal vein was exposed by ventral midline incision and a 30-gauge needle was used to administer the AAV vectors or PBS. Hemostasis was achieved by applying a cotton tipped applicator directly onto the injection site. Suture and staples were used for muscle and skin closure respectively.

D. Histopathology and immunohistochemistry

Histopathology and immunohistochemical procedures were carried out as previously described by Embury and colleagues in 2005. HBx antibody (MAB 8429, aa 50-88, Clone 146, made in mouse; Chemicon, Temecula, CA) was used for X-protein immunohistochemical detections. Sections were examined with bright-field microscopy using a Nikon Labophot-2 microscope. Microscopic images were captured with a QCLR3 3.3 million pixel QColor 3 Olympus digital camera linked to QCapture Image Pro Plus 5.1 image analysis software. For final image output, all images were processed using Adobe Photoshop CS software.

E. Genomic DNA extraction, sequencing and quantitative PCR

Genomic DNA from formalin fixed tissue samples was isolated according to manufacturers instructions using the Qiagen DNeasy Tissue Kit (Qiagen, Valencia, CA).

An RT-PCR assay and primers intended to detect HBx copy number in tumor and liver samples were designed by Seqwrite, Inc. (Houston, TX) and genomic quantitation protocols were utilized as previously described by Conlon and colleagues in 2005.

Real-time PCR (TAQMan©) was employed using the following probes and primers:

x protein 1511F:CCTGTGTTGCCACCTGGATT;
x protein 1573R:GAAGGAAGGTCCGCTGGATT; and
the TAQMan© probe x protein
1543T:ACGTCCTTCTGCTACGTC.

Sequence analysis was completed by core services at the University of Florida.

F. Western blot analysis

Frozen livers from animals receiving either AAV-WPRE (+) or WPRE (-) vectors were evaluated for the presence of HBx or PAH antigen. Cell lysates were obtained by standard methods and protein content was estimated using Bradford reagent (Bio-Rad Laboratories, CA) according to manufacturer's protocol. 20-50 µg of whole cell liver lysates per lane were resolved on 18% Tris-HCl gels and electroblotted onto nitrocellulose membranes for Western analysis by standard procedure. Conditions were optimized for antibody concentration and incubation times and found to be a primary antibody dilution of 1:500 with overnight incubation at 4° C and gentle agitation.

Initially, a chemiluminescent detection method was used with a monoclonal HBx antibody (MAB 8429, aa 50-88, Clone 146, made in mouse; Chemicon, Temecula, CA) and a custom polyclonal PAH antibody made in rabbit. These results were verified using a monoclonal anti-trp,tyr,phe hydroxylase monoclonal antibody (MAB 578; Chemicon, Temecula, CA) along with the monoclonal HBx (Chemicon, Temecula, CA) antibody with a chromogenic detection system. A 1:5000 biotinylated mouse made in horse secondary antibody with ABC Elite detection kit and DAB substrate (plus or minus nickel) (Vector Labs, Burlingame, CA) was used following overnight incubation with the primary antibody at 4°C. Tween-20 was omitted from blocking and wash steps to avoid possible interference with antibody/antigen interaction. A 10% normal horse serum in PBS solution was used for blocking and primary antibody application. All wash steps were carried out in PBS.

III. Results

To assess the clinical efficacy of increased PAH transgene expression by WPRE on *Pah^{enu2}* mice, we evaluated groups of mice treated with vectors containing the presence or absence of WPRE for 6 to 12 months. The CB-mPAH, CB-mPAH-WPRE comparison established that a WPRE-containing vector is two times more effective in lowering serum phenylalanine (Figure 1A).

At the conclusion of each study, full gross and microscopic necropsy examinations were completed on

each animal. Animals were placed into four categories according to the presence or absence of WPRE (**Table 1**). Although the vector titer required to reduce phenylalanine was reduced 2-3 fold with WPRE, we unexpectedly observed a high incidence of hepatic pathology and neoplastic disease in these animals. **Figure 1B** depicts the actual tumors that were found in WPRE treated mice. In the first group, there were 3 hepatocellular carcinomas, two hepatomas, and one hepatoblastoma. One animal in the WPRE group had both lymphoma of the spleen, intestine and mediastinal lymph node as well as adenocarcinoma of the large intestine. One mouse had a pulmonary adenocarcinoma. Overall, there were 9 tumors in 18 WPRE treated animals (50%) in the first group.

The second group was composed of 5 PKU females that received AAV5 CB-mPAH-WPRE. One animal in this group had a vertebral osteoblastic osteosarcoma.

The third group had the most unusual forms of neoplasia that included: pulmonary and splenic lymphoma, pulmonary carcinoma, intestinal carcinosarcoma, renal carcinoma and two poorly-differentiated blast-like tumors. The three groups combined had a total of 16 tumors in 36 (44%) WPRE-treated mice. There were 15 control animals that received vector that did not contain WPRE (**Table 1**). Overall, one mouse in 15 (6.6%) that did not receive WPRE had lymphoma, which we attribute to normal background incidence in aged mice.

We found unusual histologic changes in 25 out of 36 (70%)WPRE-treated livers which included hepatocyte nuclei in metaphase arrest and were not observed in non-WPRE treated animals (**Figure 1C**). The unexpected pathology in these animals was disconcerting, and from a veterinary standpoint, the author was concerned about the possible relationship between the WPRE element in the vector to the pathogenic properties of the wild-type virus.

The hepadnavirus woodchuck hepatitis virus (WHV) is known to cause chronic hepatitis and hepatocellular carcinoma in woodchucks (Tennant et al, 2004). The Hepatitis B virus (HBV) in humans is associated with similar pathology and is also a member of the family Hepadnaviridae. Both of these viruses specify a homologous gene product, known as the X-protein, which has been associated with hepatocellular carcinoma in their natural hosts (Tennant et al, 2004) and both proteins have been found to have similar properties associated with oncogenic function. Our vector contained the first 60 amino acids of the 141 amino acid WHV X-protein.

We chose to use a monoclonal Hepatitis B Virus X-protein (HBx) antibody to evaluate the presence of X-protein antigen in tissue sections due to its commercial availability. Immunohistochemical detection of X-protein antigen expression was consistently located within cells adjacent to the tumors in WPRE-treated animals, and in the bone marrow adjacent to a vertebral osteosarcoma of another WPRE-treated animal. We also found cytoplasmic HBx antigen to be present randomly and sporadically in the cytoplasm of hepatocytes from WPRE treated liver and was not detected in non-WPRE treated animals. Pulmonary macrophages and cells adjacent to pulmonary tumors displayed cytoplasmic HBx immunoreactivity (**Figure 1C,D**). The presence of X-protein antigen found systemically suggests that possibly significant amounts of widespread systemic vector dissemination occurred during portal-vein administration.

In order to determine whether AAV-vector-associated integration occurred in tumoral tissue, and more specifically, to look for the presence of HBx as a possible oncogenic stimulus, we isolated genomic DNA from formalin fixed tissues. Using qPCR, we determined that HBx DNA was present in transduced liver of WPRE-treated animals but not in control or non-WPRE-vector treated animals. WPRE-transduced liver contained between 2×10^3 to 4.4×10^4 copies per μg of DNA. The tumoral tissue showed low signal levels that were insignificant compared to the 3 to 4-fold relative increases of transduced liver samples. The qPCR results corroborated our immunohistochemical findings that Hbx antigen was detected peritumorally, but not within a large percentage of actual tumor parenchyma.

To verify the presence of X-protein antigen, frozen liver samples from WPRE treated mice were compared to samples from mice treated with non-WPRE vectors, using SDS PAGE Western blots. The X-protein fragment in our vector was 60 amino acids long, and we therefore predicted a band equivalent to 6-7 kD (**Figure 2A**). Instead, we consistently observed two bands at approximately 12 kD and 25 kD in the WPRE-treated livers when an HBx monoclonal antibody or a 37 kD band (representing a combined 12 kD and 25kD fragment) when a PAH polyclonal antibody were used (**Figure 2b**). These bands were not observed in non-WPRE liver lysates.

Table 1. Tumor incidence in WPRE-treated animals.

Group	N	Vector	Dose (Vg)	Number of Tumors
1	18 males	AAV2-mPAH-WPRE	3.7×10^9 - 1.3×10^{13}	9 (50%)
2	5 females	AAV5-mPAH-WPRE	1.3×10^{12} - 7.3×10^{13}	1 (20%)
3	13 females	AAV2-mPAH-WPRE	9×10^{11} - 3×10^{12}	6 (46%)
4	15 both	AAV2-mPAH	2×10^{11} - 1.9×10^{13}	1 (6.6%)
Total tumors from 36 WPRE treated animals				16 (44%)

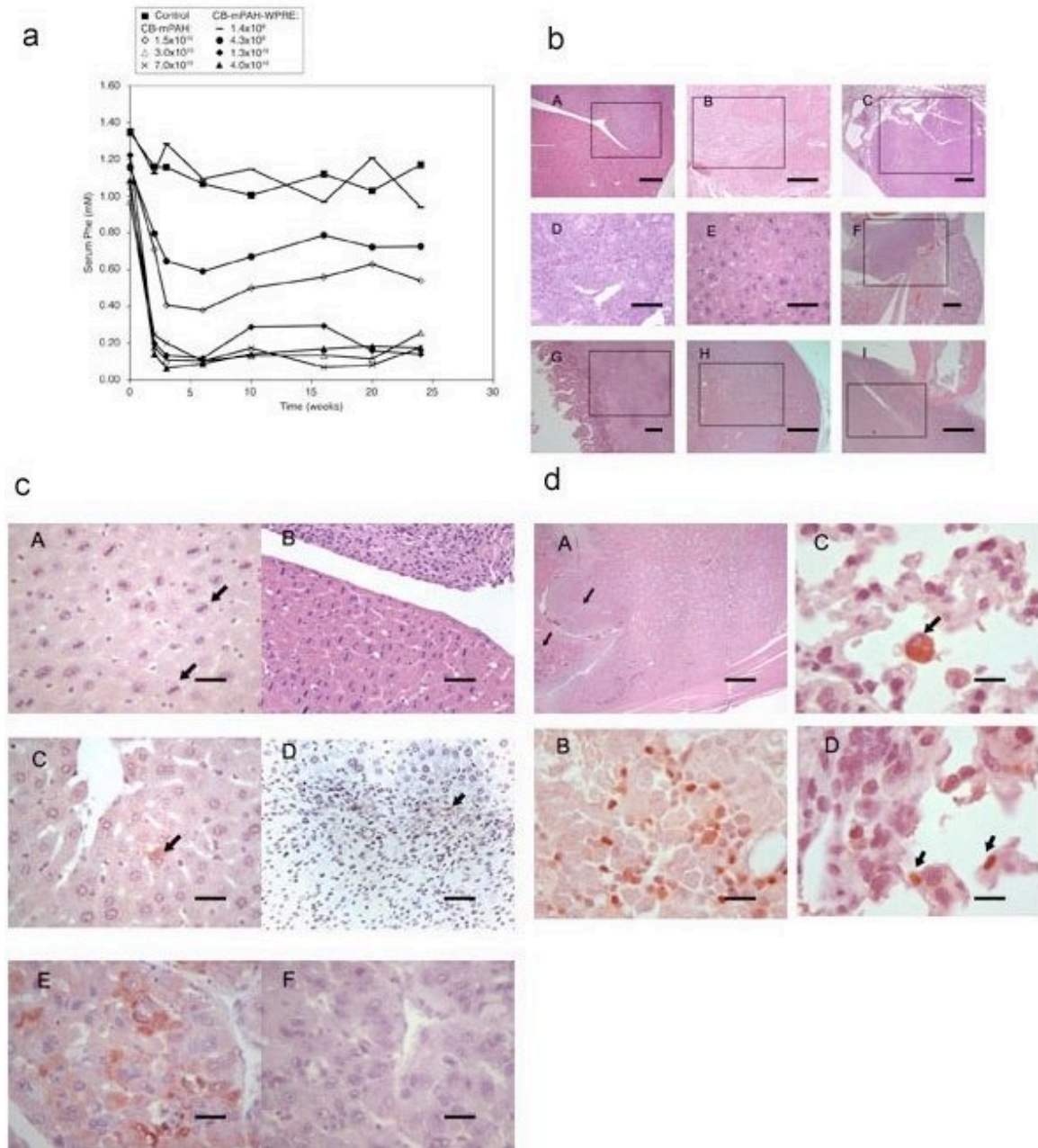


Figure 1 Serum phenylalanine levels following portal vein injections. **(a)** Normalization of serum Phe levels (below 0.2mM) was observed using 3.0×10^{10} and 7.0×10^{10} IUs of rAAV2-CB-mPAH and using 1.3×10^{10} and 4.0×10^{10} IUs of rAAV2-CB-mPAH-WPRE. The WPRE vector is twice as effective as the CB-mPAH vector in achieving phenotypic correction of the mice. Control n=2, 1.5×10^{10} CB-mPAH n=1, 3.0×10^{10} CB-mPAH n=3, 7.0×10^{10} CB-mPAH n=2, 1.4×10^9 CB-mPAH-WPRE n=3, 4.3×10^9 CB-mPAH-WPRE n=6, 1.3×10^{10} CB-mPAH-WPRE n=3, and 4.0×10^{10} CB-mPAH-WPRE n=5. **(b)** Examples of neoplasia in animals treated with AAV vectors containing WPRE. (A) Hepatoblastoma; bar=200 μ m. (B) Osteoblastic osteosarcoma; bar=100 μ m. (C) Pulmonary adenocarcinoma; bar=200 μ m. (D) Intestinal adenocarcinoma; bar=20 μ m. (E) Hepatocellular carcinoma; bar=20 μ m. (F) Mediastinal blast-like tumor; bar=200 μ m. (G) Intestinal carcinosarcoma; bar=200 μ m. (H) Renal carcinoma; bar=200 μ m. (I) Intestinal blast-like tumor; bar=200 μ m. Hematoxylin and eosin (H&E). **(c)** Hepatic pathology and X-protein antigen detection in animals treated with vector containing WPRE. (A) Metaphase arrest in hepatocytes infected with WPRE vector; bar=20 μ m, H&E. (B) Hepatocytes in metaphase arrest adjacent to a hepatoblastoma; bar=100 μ m, H&E. (C) HBx antigen is detected within cytoplasm of transduced hepatocytes; bar=20 μ m (D) HBx antigen is present within the transition between neoplastic and normal hepatocytes of the hepatoblastoma; bar=100 μ m (E) Section of human hepatocellular carcinoma used as HBx positive control; bar=10 μ m. (F) Human hepatocellular carcinoma HBx negative control (denotes the absence of non-specific background staining); bar=10 μ m. HBx immunoperoxidase method, hematoxylin counterstain. **(d)** HBx antigen detection in cellular elements adjacent to neoplasms of WPRE-treated animals. (A) Arrows depict region of bone marrow adjacent to a vertebral osteoblastic osteosarcoma that displays HBx antigen; bar=100 μ m, H&E. (B) High magnification of bone marrow cells reveal HBx immunopositivity; bar=10 μ m. (C) HBx immunopositive pulmonary macrophage adjacent to pulmonary tumor; bar=10 μ m. (D) Cytoplasmic inclusions demonstrate immunopositivity for HBx antigen in peripheral cells adjacent to pulmonary adenocarcinoma; bar=10 μ m. HBx immunoperoxidase method, hematoxylin counterstain.

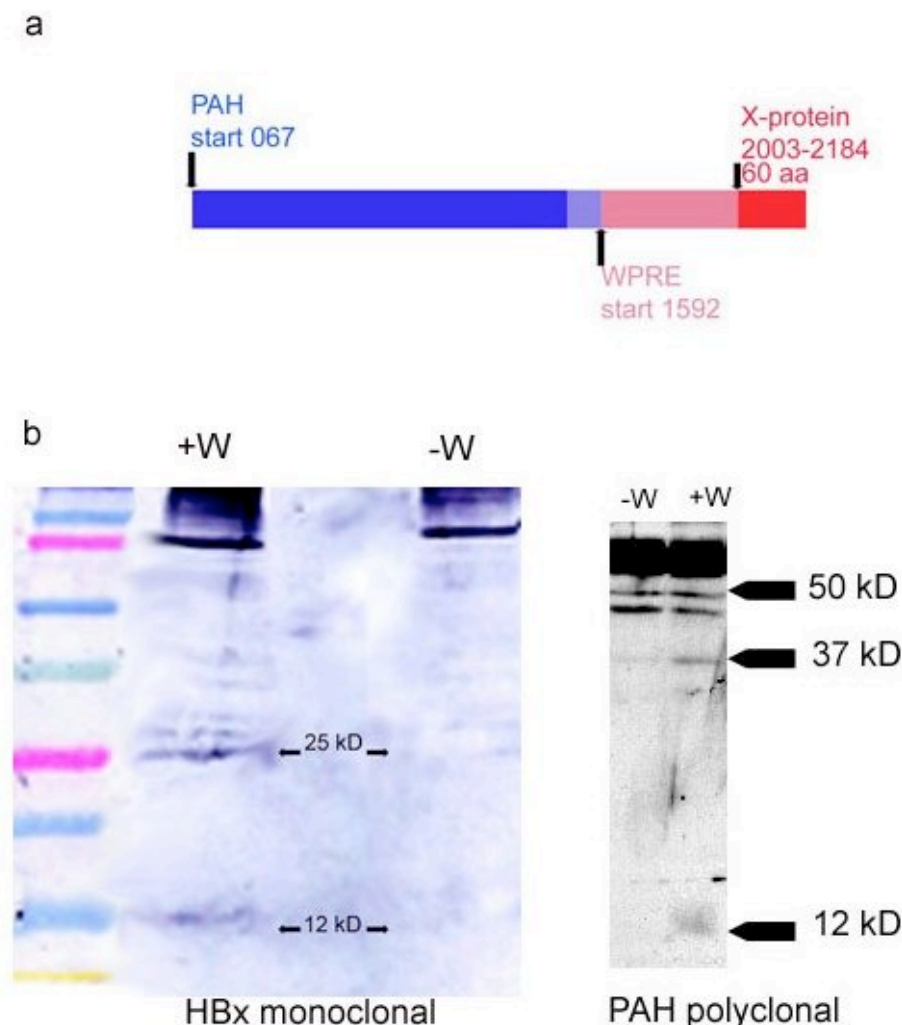


Figure 2 Antigen detection in liver lysates of animal treated with AAV-WPRE vectors.

(a) Schematic diagram of the PAH transgene and WPRE in the vector element shows the relative location and size of the 60 aa X-protein fragment. (b) The expected band at 6-7 kD was not present in WPRE treated animals, however, bands at approximately 12 and 25 kD are present using an HBx monoclonal antibody. A band at 12 kD is evident with a PAH monoclonal antibody but the 25 kD band is not readily apparent. However, there is a band at 37 kD which may represent a combined unit protein of the 12 and 25 kD protein fragments. The 50 kD band represents endogenous PAH in both the treated and non-treated animals. Bands at 12, 25 or 37 kD are not detected in non-WPRE treated animals.

Computer analysis of the vector sequence suggested that possible alternative splice sites could result in the 12 and 25 kD protein bands. Two splice donor sites were located in the PAH transgene (D3 and D4), and 1 splice acceptor (A3) was located within the X-protein fragment of the WPRE element (**Figure 3a**). The two possible fusion proteins of 12 kDa and 25 kDa corresponded to the sizes seen in our western blots. A single PAGE gel was immunoblotted and cut in half. One half of the membrane was incubated with HBx monoclonal antibody, and the remaining half was incubated with PAH polyclonal antibody revealing identical bands at approximately 12 kD and 25 kD. The native PAH protein is approximately 50 kD, and was confirmed on the PAH incubated membrane but not the HBx incubated membrane (**Figure 3b**).

An attempt to retrieve RNA transcripts of the fusion construct from WPRE-treated livers, the hepatoblastoma,

the hepatocellular carcinoma, peritoneal mesothelioma, and mediastinal mesothelioma embedded in paraffin blocks was made using RecoverAll™ (Ambion, Austin, TX). 3-4 sections (20-30 mg) of each tissue were removed from each block and deparaffinized. The isolation protocol was followed according to the manufacturer's recommendation. The RNA samples were run out on gels, however, all lanes contained streaks of degraded RNA. Perera's laboratory at the USDA also attempted RNA isolation of the paraffin embedded tissues, as well as frozen liver tissue samples with similar results of degraded RNA. Currently, we have transfected normal liver cells with our original mPAH-WPRE expression plasmid used in the AAV vector. RNA isolation from these cells was successful in terms of quantity and quality, and these samples are currently being analyzed for the presence of fusion transcripts using qPCR.

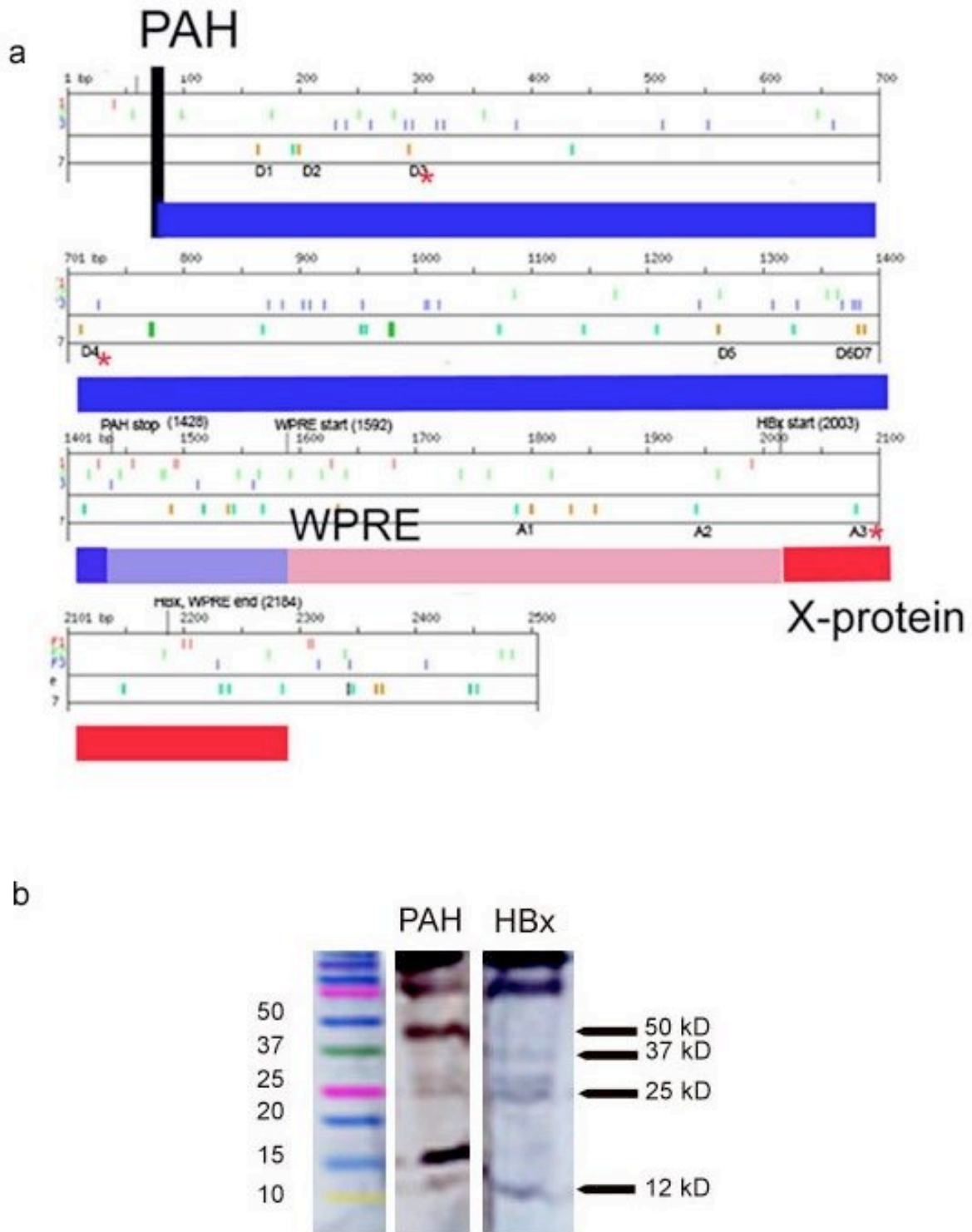


Figure 3 Schematic fusion protein diagram with corresponding western blot analysis. **(a)** Computer analysis revealed two splice donor sites were located in the PAH transgene (D3=75 aa, D4= 139 aa), and 1 splice acceptor (A3=35 aa) within the WPRE element . A D3+A3 splice would result in 110 aa (12.1 kD). A continuous fragment composed of D3+D4+A3 splice would result in 249 aa (25 kD) **(b)** Identical bands at 12 kD and 25 kD were present when the membrane was cut in half and incubated with either HBx or PAH polyclonal antibody.

IV. Discussion

Although this is essentially a retrospective clinical study, we submit this fusion protein is a likely candidate for the increased tumor incidence seen in WPRE vector

treated mice. The X-protein encodes two separate functional domains, a regulatory domain and a transacting domain. The ser/pro-rich regulatory domain (aa 21-50) is the minimal region for strong homologous association and autoregulation of expression (Murakami et al, 1994). Our

vector contained the first 60 amino acids of the WHV X-protein, therefore this auto-regulator of X-protein expression was included in our vector. Although our X-protein sequence was modified with the intention of preventing expression, it is probable these modifications were by-passed in favor of the alternative splice sites.

Our qPCR and immunohistochemical results reveal that X-antigen was located primarily on the periphery of tumors or sporadically within individuals cells located within the tumors themselves. We speculate that these tumors were not caused by viral integrative events resulting in clonal expansion of a transformed cell. If that were the case, the majority of the tumor would contain X-antigen. Rather, we surmise that the AAV vector entered the systemic circulation and localized to occasional cells throughout the body. The X-protein is capable of activating numerous translational events on various oncogenes such as c-myc and fas. We speculate that individual cells became transformed by the X-protein, acting in a hit and run fashion initiating downstream transformational events and tumor formation.

The X-protein has been shown to modulate a wide variety of viral and cellular transcriptional elements as well as cell cycle progression, apoptosis and DNA repair (Doria et al, 1995; Melegari et al, 1998; Bouchard and Schneider, 2004; Branda and Wands, 2006). Many of these activities occur through HBx -mitochondrial interactions influencing calcium regulation of downstream oncogenic signaling cascades (Bouchard et al, 2001). Extensive functional mapping studies have determined that the carboxy-terminal region of HBx influences its interactions with mitochondria (Huh and Siddiqui, 2002; Shirakata and Koike, 2003), and its absence is implicated in tumorigenesis of hepatocellular carcinoma (Wei et al, 1995; Hsia et al, 1997; Wollersheim et al, 1988; Poussin et al, 1999; Chen et al, 2000; Tu et al, 2001). One of the fundamental activities of HBx is modulation of cellular calcium levels and subsequent activation focal adhesion kinase (Pyk2/FAK) and Src kinases. Calcium signaling and activation of Pyk2/FAK are the starting points for many complex signaling pathways and a large number of these pathways lead to neoplastic transformation. Therefore, integration and clonal expansion would not be necessary for induction of transformation in this particular scenario.

Most, if not all X-protein sequences isolated from HBx genomes in tumor tissue have been found to have a deletion of the carboxy terminal 3' end (Tu et al, 2001). Interestingly, the vector used in our study contained a carboxy-terminal truncation, which may have inadvertently conferred additional pathogenicity to our vector.

One cannot generalize about single common features regarding gene therapy or treatment for other genetic diseases that may result in adverse side effects. Every model must be considered on an individual basis. Each strain of transgenic mouse, each transgene, and each vector have different characteristics. Therefore, every model will have its own unique synergistic features. It may not always be possible to predict exactly the way one system will behave. These results have important

implications for many scientific disciplines. In a letter to the editor in the journal *Gene Therapy* in 2005, Kingsman warned of the possibility that the X-protein may retain biologic activity potentially related to tumor development (Poussin et al, 1999). They modified their WPRE to prevent expression of X-protein fragments. Safety issues for laboratory personnel and the general well-being of laboratory animals receiving genetic material containing WPRE should be taken into consideration, as well as its use in the treatment of genetic diseases.

Acknowledgements

This study was supported by NIH/NCRR grant K01RR0119979. Necropsy evaluations and pathologic diagnoses were made by JE. Immunohistochemistry was performed by J.E. Experiments were designed by J.E., P.L., S.F., C.C., O.P., R.C. and T.F. Vector was made by the Vector Core Laboratory, Powell Gene Therapy Center, University of Florida. Surgeries were performed by C.C. and P.L. pCR analysis was by O.P, A.Z, A.P, R.C, and T.F. Western blot procedures and analysis were completed by J.E., S.F., and E.M. The manuscript was written by J.E.

References

- Bouchard MJ, Schneider RJ (2004) The enigmatic X gene of hepatitis B virus. **J Virol** 78, 12725-12734.
- Bouchard MJ, Wang LH, Schneider RJ (2001) Calcium signaling by HBx protein in hepatitis B virus DNA replication. **Science** 294, 2376-2378.
- Branda M, Wands JR (2006) Signal transduction cascades and hepatitis B and C related hepatocellular carcinoma. **Hepatology** 43, 891-902.
- Chen WN, Oon CJ, Leong AL, Koh S, Teng SW (2000) Expression of integrated hepatitis B virus X variants in human hepatocellular carcinomas and its significance. **Biochem Biophys Res Commun** 276, 885-892.
- Conlon TJ, Cossette T, Erger K, Choi YK, Clarke T, Scott-Jorgensen M, Song S, Campbell-Thompson M, Crawford J, Flotte TR (2005) Efficient hepatic delivery and expression from a recombinant adeno-associated virus 8 pseudotyped alpha1-antitrypsin vector **Mol Ther** 12, 867-875.
- Donello JE, Loeb JE, Hope TJ (1998) Woodchuck hepatitis virus contains a tripartite posttranscriptional regulatory element. **J Virol** 72, 5085-5092.
- Doria M, Klein N, Lucito R, Schneider RJ (1995) The hepatitis B virus HBx protein is a dual specificity cytoplasmic activator of Ras and nuclear activator of transcription factors. **EMBO J** 14, 4747-4757.
- Embury JE, Reep RR, Laipis PJ (2005) Pathologic and immunohistochemical findings in hypothalamic and mesencephalic regions in the pah(enu2) mouse model for phenylketonuria. **Pediatr Res** 58, 283-287.
- Hsia CC, Nakashima Y, Tabor E (1997) Deletion mutants of the hepatitis B virus X gene in human hepatocellular carcinoma. **Biochem Biophys Res Commun** 241, 726-729.
- Huh KW, Siddiqui A (2002) Characterization of the mitochondrial association of hepatitis B virus X protein, HBx. **Mitochondrion** 1, 349-359.
- Kingsman SM, Mitrophanous K, Olsen JC (2005) Potential oncogene activity of the woodchuck hepatitis post-transcriptional regulatory element WPRE. **Gene Ther** 12, 3-4.
- Loeb JE, Cordier WS, Harris ME, Weitzman MD, Hope TJ (1999) Enhanced expression of transgenes from adeno-

- associated virus vectors with the woodchuck hepatitis virus posttranscriptional regulatory element: implications for gene therapy. **Hum Gene Ther** 10, 2295-2305.
- Mccaman MW, Robins E (1962) Fluorimetric Method for Determination of Phenylalanine in Serum. **J Lab Clin Med** 59, 885-890.
- McDonald JD, Charlton CK (1997) Characterization of mutations at the mouse phenylalanine hydroxylase locus. **Genomics** 39, 402-405.
- Melegari M, Scaglioni PP, Wands JR (1998) Cloning and characterization of a novel hepatitis B virus x binding protein that inhibits viral replication. **J Virol** 72, 1737-1743.
- Murakami S (1999) Hepatitis B virus X protein: structure, function and biology. **Intervirology** 42, 81-99.
- Murakami S, Cheong JH, Kaneko S (1994) Human hepatitis virus X gene encodes a regulatory domain that represses transactivation of X protein. **J Biol Chem** 269, 15118-15123.
- Poussin K, Dienes H, Sirma H, Urban S, Beaugrand M, Franco D, Schirmacher P, Bréchet C, Paterlini Bréchet P (1999) Expression of mutated hepatitis B virus X genes in human hepatocellular carcinomas. **Int J Cancer** 80, 497-505.
- Scriver CR (1995) *The metabolic and molecular bases of inherited disease*(McGraw-Hill, Health Professions Division, New York.
- Shedlovsky A, McDonald JD, Symula D, Dove WF (1993) Mouse models of human phenylketonuria. **Genetics** 134, 1205-1210.
- Shedlovsky A, McDonald JD, Symula D, Dove WF (1993) Mouse models of human phenylketonuria. **Genetics** 134, 1205-1210.
- Shirakata Y, Koike K (2003) Hepatitis B virus X protein induces cell death by causing loss of mitochondrial membrane potential. **J Biol Chem** 278, 22071-22078.
- Song S, Embury J, Laipis PJ, Berns KI, Crawford JM, Flotte TR (2001) Stable therapeutic serum levels of human alpha-1 antitrypsin (AAT) after portal vein injection of recombinant adeno-associated virus (rAAV) vectors. **Gene Ther** 8, 1299-1306.
- Tennant BC, Toshkov IA, Peek SF, Jacob JR, Menne S, Hornbuckle WE, Schinazi RD, Korba BE, Cote PJ, Gerin JL (2004) Hepatocellular carcinoma in the woodchuck model of hepatitis B virus infection. **Gastroenterology** 127, S283-S293.
- Tu H, Bonura C, Giannini C, Mouly H, Soussan P, Kew M, Paterlini-Bréchet P, Bréchet C, Kremsdorf D (2001) Biological impact of natural COOH-terminal deletions of hepatitis B virus X protein in hepatocellular carcinoma tissues. **Cancer Res** 61, 7803-7810.
- Wei Y, Etiemble J, Fourel G, Vitvitski-Trepo L, Buendia MA (1995) Hepadna virus integration generates virus-cell cotranscripts carrying 3' truncated X genes in human and woodchuck liver tumors. **J Med Virol** 45, 82-90.
- Wollersheim M, Debelka U, Hofschneider PH (1988) A transactivating function encoded in the hepatitis B virus X gene is conserved in the integrated state. **Oncogene** 3, 545-552.
- Zufferey R, Donello JE, Trono D, Hope TJ (1999) Woodchuck hepatitis virus posttranscriptional regulatory element enhances expression of transgenes delivered by retroviral vectors. **J Virol** 73, 2886-2892.



Jennifer E. Embury